Journal of Statistical Physics, Vol. 36, Nos. 5/6, 1984

Transport in a Disordered One-Dimensional System: A Fractal View

Robert J. Rubin[1]

We reexamine the calculation of the transmission coefficient of a random array of N isotopic defects in an otherwise perfect, harmonic, one-dimensional crystal lattice. The thermal conductivity of this model system has been studied under steady state conditions in which there is a kinetic temperature difference across, and an associated energy flux through, the array of defects. An exact expression for the transmission coefficient is obtained in terms of the magnitude of an Nth-order determinant. Rubin reduced the evaluation of the determinant to the evaluation of a sequence of $N-1$ nonlinear transformations drawn from a set of transformations parametrized by the nearest-neighbor spacing of the isotopic defects. These transformations are self-inverse and provide an example of what Mandelbrot has termed a *self-inverse fractal.* The variety of limiting distributions of values obtained under these transformations will be illustrated.

KEY WORDS: Disordered harmonic crystal; energy transport; fractional linear transformation; localization; self-inverse fractal; transmission coefficient.

1. INTRODUCTION

This paper is devoted to the study of a set of random fractional linear transformations which appears in a model for studying energy transport in a disordered system.[1-6] These transformations are self-inverse and provide an example of what Mandelbrot[7] has termed a *self-inverse fractal.* We will first describe the physical model and summarize known analytic results which are used in this paper.[1,2] Then we will present some results, based on Monte Carlo simulations of the disorder, which illustrate the variety of limiting behavior encountered in iterating fractional linear transformations which are selected at random from a particular set.

[1] Polymers Division, National Bureau of Standards, Gaithersburg, Maryland 20899.

0022-4715/84/0900-0615$03.50/0

2. THE MODEL

We consider an infinite one-dimensional harmonic crystal with nearest-neighbor interactions. The particles are labeled by the index r, $-\infty < r < \infty$; and all particles have the mass m except for N defect particles at lattice positions $r = A_j$, $j = 1,..., N$. The mass of each of the defect particles is M; and the nearest-neighbor force constant is assumed to be equal to f everywhere in the crystal, independent of local values of particle mass. It is assumed that $0 = A_1 < A_2 < \cdots < A_N$ and that nearest-neighbor spacings, $A_n = A_n - A_{n-1}$, are independent, identically distributed random variables. The equations of motion of the one-dimensional crystal are

$$(m_r/m)\,\chi_{\tau\tau}(r,\tau) = \tfrac{1}{4}[\chi(r-1,\tau) - 2\chi(r,\tau) + \chi(r+1,\tau)] \tag{1}$$

where $\chi(r,\tau)$ is the displacement of particle r from its equilibrium position and m_r is the mass of the particle at lattice site r. In Eq. (1), τ is a dimensionless time $\tau = 2(f/m)^{1/2}t$; and each subscript τ denotes differentiation with respect to τ.

The transport problem which we consider in this model is the calculation of the steady state transmitted amplitude, T_N, of a wave of frequency ω in the region $r > A_N$ when a wave of unit amplitude and frequency ω is incident on the disordered region from the left. In the infinite perfect crystal [all $m_r = m$ in Eq. (1)], a unit-amplitude wave of frequency ω moving from left to right is

$$\chi(r,\tau) = \exp[i(\omega\tau - kr)] \tag{2}$$

with the frequency $\omega = \sin(k/2)$. Rubin[1] obtained the following explicit expression for the transmitted amplitude of a particle at $r \geqslant A_N$:

$$T_N = |D_n|^{-1} \tag{3}$$

where D_N denotes the determinant of the matrix whose (r,s) element is

$$\{\delta_{r,s} + i\Delta \exp[-ik\,|A_r - A_s|]\} \tag{4}$$

where $\delta_{r,s}$ is the Kronecker delta,

$$\Delta = Q\omega(1-\omega^2)^{-1/2} \tag{5}$$

and

$$Q = (M/m) - 1 \tag{6}$$

The determinant D_N can be reduced to tridiagonal form so that D_N satisfies a two-term recurrence relation

$$D_N = [1 + i\Delta + (1 - i\Delta)\exp(-2ika_N)]D_{n-1} - \exp(-2ika_N)D_{n-2} \quad (7)$$

with $D_0 = 1$, $D_1 = 1 + i\Delta$ and $a_n = A_n - A_{N-1}$. This relation is equivalent to the linear fractional transformation

$$g_N = [\delta + (\delta - g_{N-1})\exp(-2ika_N - 2i\phi)]^{-1} \quad (8)$$

where $g_N = e^{i\phi}D_{N-1}/D_N$, $1 + i\Delta = \delta e^{i\phi}$, and $g_1 = \delta^{-1}$. The transmitted amplitude for a single defect is

$$T_1 = \delta^{-1}$$

In the limit of very low concentration of defects, i.e., when the mean nearest-neighbor spacing is large compared to incident wave length, Rubin[1] has shown that the defects in a random array scatter independently, and

$$T_N = T_1^N$$

Specifically, in the limit $a = \langle a_n \rangle \to \infty$, and $\omega = \sin(k/2)$ with k different from a rational fraction of π,

$$\lim_{N\to\infty} \frac{1}{N} \ln T_N = -\ln \delta$$

Rubin defined the attenuation per defect, $\alpha_N(\omega, Q, a)$, as

$$\alpha_N(\omega, Q, a) = -\frac{1}{N} \ln T_N \quad (9)$$

This quantity is simply related to the localization length, which has been the subject of many investigations[1-4,6,8] of transport in disordered systems. Assuming that the nearest-neighbor spacing distribution function has the form

$$p(a_n) = c(1 - c)^{a_n - 1}, \qquad a_n = 1, 2, \ldots \quad (10)$$

with $a = \langle a_n \rangle = c^{-1}$, Rubin[1] evaluated $\alpha_N(\omega, Q, a)$. A typical set of results is shown in Fig. 1 where values of $\alpha_N(\omega, Q, a)$ are plotted as a function of ω in the case $Q = 1$, $a = 10$ for arrays of $N = 3 \times 10^4$ defects. Each point represents a value of $\alpha_N(\omega, 1, 10)$ for a different random array of defects. Values of $\alpha_N(\omega, 1, 10)$ for different random arrays, but the same frequency,

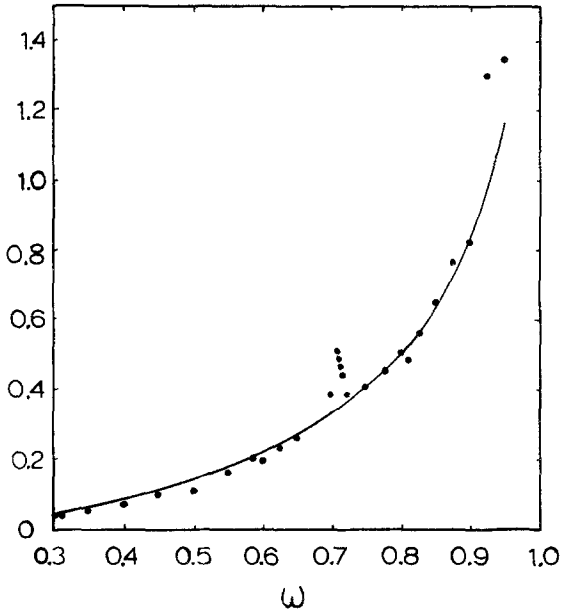

Fig. 1. Plot of the Monte Carlo estimates of $\alpha_N(\omega, 1, 10)$ based on arrays of 3×10^4 defects. The dots represent the values of $\alpha_N(\omega, 1, 10)$. The solid curve is a plot of ln δ, the attenuation constant for a single isolated defect.

are indistinguishable on the scale of Fig. 1. The solid curve in Fig. 1 is a plot of the function

$$-\ln T_1 = \ln \delta$$

the attenuation of independent scatterers. This function provides a surprisingly good fit to the results of the simulations for $a \geqslant 10$ and $\omega \leqslant 0.9$.

Our interest in this paper lies in the connection between the structure evident, in Fig. 1, in values of $\alpha_N(\omega, 1, 10)$ near $\omega \cong 0.5$, 0.6, 0.7, and 0.8 and the structure in the related distribution of values of $\{g_n\}$. The general relation between these quantities, $\alpha_N(\omega, Q, a)$ in Eq. (9) and the g_n's defined in Eq. (8), is

$$\alpha_N(\omega, Q, a) = -N^{-1} \sum_{n=1}^{N} \ln |g_n| \tag{11}$$

Structure in the distribution of the values of sets of $\{g_n\}$ obtained for disordered arrays of defects will be illustrated in Section 3.

In addition to the formula for T_N, one can obtain[1] an explicit expression for the physically related ratio of the amplitude of the last defect particle at A_n to the amplitude of the first defect particle at A_1,

$$\begin{aligned} \tilde{T}_N &= |\chi(A_N)|/|\chi(A_1)| \\ &= |\tilde{D}_N|^{-1} \end{aligned} \tag{12}$$

The determinant $\tilde{D}_N$ satisfies the same two-term recurrence relation as D_N, Eq. (7), but with the different starting conditions: $\tilde{D}_0 = 1$, $\tilde{D}_1 = 1$. Consequently, the linear fractional transformation for $\tilde{g}_n = e^{\phi i}\tilde{D}_{N-1}/\tilde{D}_n$ is that for g_N in Eq. (8) with $\tilde{g}_1 = e^{\phi i}$. Rubin[2] showed, by combining the recurrence relations for D_N and $\tilde{D}_N$, that

$$g_N - \tilde{g}_N = i\Delta \exp(\phi i - 2kA_N i) T_N \tilde{T}_N \tag{13}$$

It follows from Eq. (13) that whenever T_N and $\tilde{T}_N \to 0$ with increasing N, $g_N - \tilde{g}_N \to 0$.

Finally, consider the complex g plane depicted in Fig. 2 and the transformation

$$g = [\delta + (\delta - g')e^{-2ika - 2i\phi}]^{-1}$$

where $\delta = |1 + i\Delta| = (1 + \Delta^2)^{1/2}$ and $\phi = \tan^{-1}\Delta$. The unit circle C has its center at the origin and the orthogonal circle K_0 with radius $|\Delta|$ has its center at $(\delta, 0)$. The vector g' defines a circle K, concentric with K_0. The

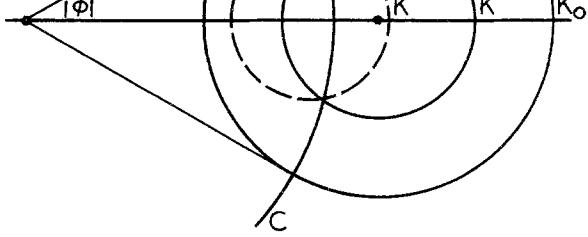

Fig. 2. The complex g plane showing the unit circle C with its center at the origin and the circles K and K_0 with their centers at δ. The circle K' is the inverse of the circle K in the unit circle.

vector $\delta + (\delta - g')e^{-2ika-2i\phi}$ also lies on K. The image of the circle K in the unit circle C is also a circle,[9] and is shown dashed in Fig. 2. It the vector $\rho e^{i\beta}$ lies on K, then its reciprocal, or image in the unit circle, is $\rho^{-1}e^{-i\beta}$; and it lies on K'. The circle K_0, which is othogonal to the unit circle is self-reciprocal.[9] The initial value, $g_1 = \delta^{-1}$, lies inside the unit circle on the real axis, whereas the initial value, $\tilde{g}_1 = e^{i\phi}$, lies at an intersection of K_0 and C. (The particular intersection is determined by the algebraic sign of Q.) Thus the distribution of successive values of $\tilde{g}_n$ associated with a particular array of defects lies on the circle K_0 whereas the successive values of g_n lie in the interior of K_0.

3. RESULTS OF SIMULATION EXPERIMENTS

The attenuation, $\alpha_N(\omega, Q, a)$, which is defined in Eq. (9) as the average of $\ln|g_n|$, is a function of three parameters besides N whose ranges are $0 < \omega < 1$, $-1 < Q < \infty$, and $1 < a < \infty$. In Fig. 3, we have plotted the values of g_n inside the circle K_0 for $n = 1,..., 10^4$ in the case $\omega = 0.1$, $Q = -0.2$, with nearest-neighbor spacings between defects selected according to the distribution, Eq. (10) when $\langle a \rangle = 10$. The value of $\phi = \tan^{-1} \Delta$ in this case is $\phi \cong -0.02$ radians. Thus the angle $2|\phi|$ subtended by the circle K_0 at the center of the unit circle (see Fig. 2) is relatively small. The results of a different simulation in which only the value of $\langle a \rangle$ has been changed are shown in Fig. 4. In this case $\langle a \rangle = 2$. One piece of information which is necessarily suppressed in the representation of the values of the large number

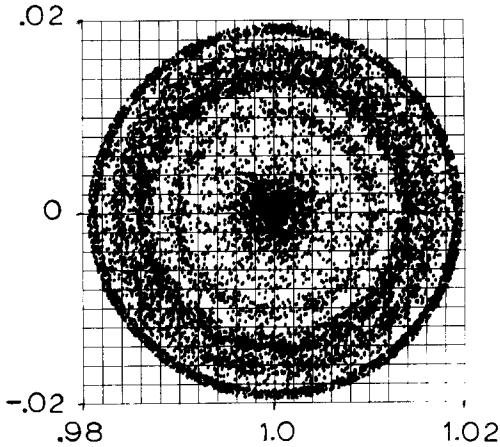

Fig. 3. Plot of locations of 10^4 values values of g_n inside the circle K_0 for the case $\omega = 0.1$, $Q = -0.2$, and $\langle a \rangle = 10$.

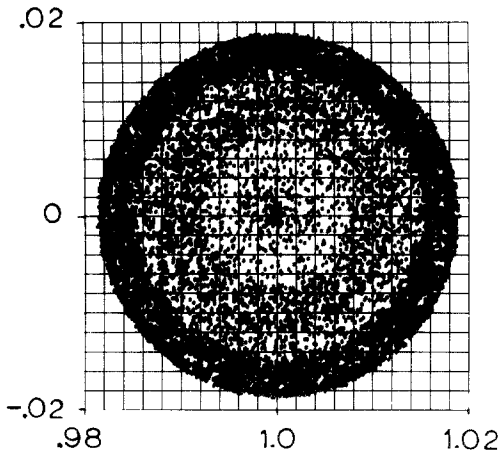

Fig. 4. Plot of locations of 10^4 values of g_n inside the circle K_0 for the case $\omega = 0.1$, $Q = -0.2$, and $\langle a \rangle = 2$.

of g_n's in Figs. 3 and 4 is their order in the sequence of generation. Suffice it to say that the next 10^4 values of g_n in either case lie in a narrow annular ring close to the limiting circle, K_0. For larger values of $|\phi| = |\tan^{-1} \Delta|$, similar plots of the distribution of the first 10^4 values of g_n inside the circle K_0 are characterized by a sparse set of points in the interior of K_0 with the majority of points lying close to the boundary circle K_0. It follows from Eq. (13) as well as test simulations that g_n approaches $\tilde{g}_n$ for large n. Consequently, a prominent feature in the values of $\alpha_N(\omega, 1, 10)$ such as that near $\omega = 0.7$, can as readily be related to the distribution of values of $\tilde{g}_n$ as to the distribution of values of g_n. Rubin[1] showed that the successive values of $\tilde{g}_n$ for $\omega = \sin(\pi/4)$, i.e., $k = \pi/2$, and $Q \geqslant 1$ all lie on the portion of the circumference of K_0 which lies *inside* the unit circle. In this case the circle K_0 subtends the angle $2\phi \geqslant \pi/2$ at the center of the unit circle. For values of k close to, but different from, $\pi/2$ the values of $\tilde{g}_n$ spill out into the remainder of the circumference of K_0. In Fig. 5 we have represented the distribution of 10^4 values of $\tilde{g}_n$ on the circumference of K_0 inside the unit circle in the case $k = \pi/2$, $Q = 1$ and $\langle a \rangle = 8/3$. This portion of the circumference has been divided into 501 equal intervals and the fraction of $\tilde{g}_n$ values which fall in each interval is plotted vs. the interval number. The restricted range of the g transformation in this case can be easily demonstrated[1,2] because the rotation factor $\exp(-2ika_n - 2i\phi)$, which rotates the difference $\delta - \tilde{g}_{n-1}$ on the circumference of the circle K_0, assumes only two values depending upon whether a_n is odd or even, respectively, $\exp(i\pi/2)$ or $\exp(-i\pi/2)$. The relative frequency with which these two rotation factors occur is related to the value

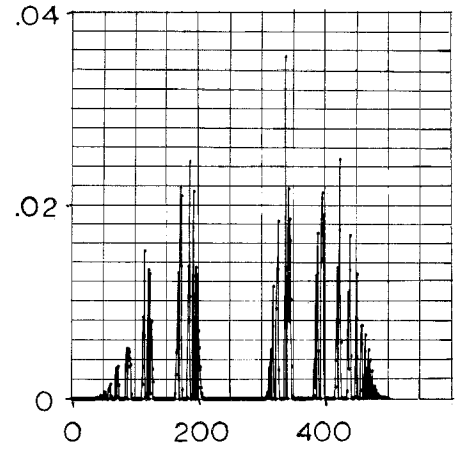

Fig. 5. Plot of the distribution of 10^4 values of $\tilde{g}_n$ on the arc of K_0 inside the unit circle in the case $\omega = 2^{-1/2}$, $Q = 1$, $\langle a \rangle = 8/3$. The arc has been divided into 501 equal intervals and the fraction of the values of $\tilde{g}_n$ contained in each interval is plotted vs. interval number.

of $\langle a \rangle$. Either of the $\pi/2$ rotation factors carries the $\pi/2$ interior arc of K_0 outside the unit circle so that there is a gap between the two resultants. When the inverse of a resultant is formed in the unit circle to complete the g transformation, the new value of g lies on K_0 inside the unit circle.[1] Since all values of $\tilde{g}_n$ lie inside the unit circle, the value of

$$\tilde{a}_N(2^{-1/2}, 1, a) = -N^{-1} \sum_{n=1}^{N} \ln |\tilde{g}_n|$$

is obviously positive. The prominent peak in the values of $a_N(\omega, 1, 10)$ in Fig. 1 near $\omega = 2^{-1/2}$ can be understood as a consequence of the spilling out of values of $\tilde{g}_n$ from inside the unit circle to cover the entire circle K_0 as ω departs from the value $2^{-1/2}$ and an associated reduction in the value of the sum

$$-N^{-1} \sum_{n=1}^{N} \ln |\tilde{g}_n|$$

Finally, in Figs. 6 and 7, we show the distribution of 10^4 values of $\tilde{g}_n$ on the circle K_0 for the cases $w = \sin(\pi/6)$, $(k = \pi/3)$, $Q = 1$, $\langle a \rangle = 2$ and $\omega = \sin(\pi/5)$, $(k = 2\pi/5)$, $Q = 1$, $\langle a \rangle = 2$. In both cases the circumference of K_0 has been divided into 301 equal intervals, labeled from 0 to 300. Intervals

[1] Subsequent iterations of the two transformations produce the gaps within gaps within gaps, as seen in Fig. 5 and typical of fractal structures.

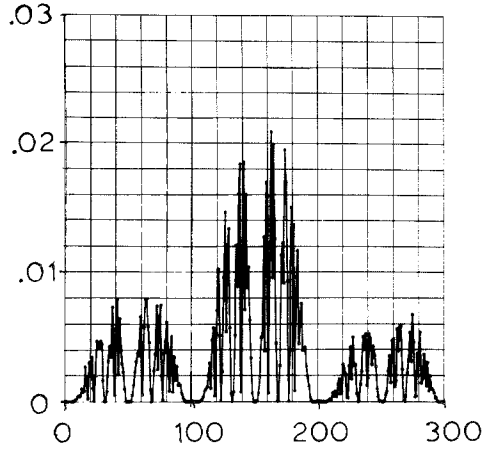

Fig. 6. Plot of the distribution of 10^4 values of $\tilde{g}_n$ on the circle K_0 in the case $\omega = 1/2$, $(k = \pi/3)$, $Q = 1$, $\langle a \rangle = 2$. The circumference of K_0 has been divided into 301 equal intervals labeled from 0 to 300 and the fraction of the values of $\tilde{g}_n$ contained in each interval is plotted vs. interval number. Intervals 0 and 300 are farthest from the center of the unit circle.

0 and 300 are farthest from the center of the unit circle. The fraction of $\tilde{g}_n$ values in each interval is plotted versus interval number. There is considerable structure evident in the distribution of $\tilde{g}_n$ values in each of these figures as well as that in Fig. 5 for $\omega = \sin(\pi/4)$, $(k = \pi/2)$, $Q = 1$, $\langle a \rangle = 8/3$. The gaps in the $\tilde{g}_n$ distributions are striking. However, except for the peak in the $\alpha_N(\omega, 1, 10)$ distribution near $\omega = 2^{-1/2}$, we have not as yet been able to establish any simple relationship between structure in $\tilde{g}_n$ distributions and

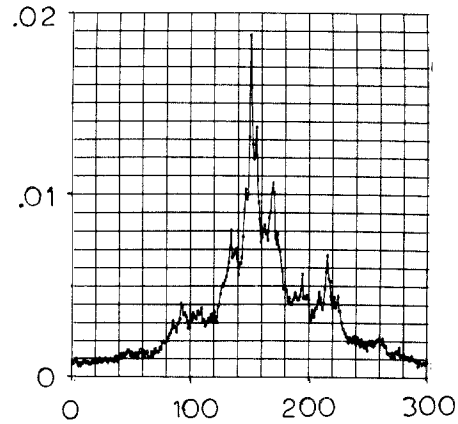

Fig. 7. Plot of the distribution of 10^4 values of $\tilde{g}_n$ on the circle K_0 in the case $\omega = \sin(\pi/5)$, $(k = 2\pi/5)$, $Q = 1$, $\langle a \rangle = 2$.

some of the less-pronounced features in the plot of $\alpha_N(\omega, 1, 10)$ vs. ω in Fig. 1. Further study of the g transformations is of interest, independent of their connection with attenuation in the transmission problem. In the examples depicted in Figs 5–7, members of a set of transformations which differ only in the values of the spacings, a_n, have different fixed points. Thus repeated iteration with a particular set member leading to convergence toward its fixed point is interrupted whenever a different member of the set of transformations is introduced into the sequence. Is this repeated interruption a sufficient condition for gaps and/or structure in the $\tilde{g}_n$ distribution? In the foregoing examples, the parameter $k = 2 \sin^{-1} \omega$ is a rational fraction of π; and consequently the number of members of the associated set of g transformations is finite.

ACKNOWLEDGMENT

The Monte Carlo simulations reported here are samples of an extensive investigation carried out with the assistance of Mrs. Mary Menzel at the Los Alamos Scientific Laboratory.

REFERENCES

1. R. J. Rubin, *J. Math. Phys.* **9**:2252 (1968).
2. R. J. Rubin, *J. Math. Phys.* **11**:1857 (1970).
3. R. J. Rubin and W. L. Greer, *J. Math. Phys.* **12**:1686 (1971).
4. A. Casher and J. L. Lebowitz, *J. Math. Phys.* **12**:1701 (1971).
5. R. J. Rubin, in *Perspectives in Statistical Physics*, H. J. Raveché, ed. (North-Holland Publishing Co., Amsterdam, 1981), pp. 111–112).
6. W. M. Visscher, *Methods Comput. Phys.* **15**:371 (1976).
7. B. B. Mandelbrot, *The Fractal Geometry of Nature* (W. H. Freeman and Co., San Francisco, 1982).
8. P. W. Anderson, *Phys. Rev.* **109**:1492 (1958); R. E. Borland, *Proc. R. Soc. A* **274**:519 (1963); H. Matsuda and K. Ishii, *Prog. Theor. Phys. Suppl.* **45**:56 (1970); K. Ishii, *Prog. Theor. Phys. Suppl.* **53**:77 (1973); A. J. O'Connor and J. L. Lebowitz, *J. Math. Phys.* **15**:692 (1974); A. J. O'Connor, *Commun. Math. Phys.* **45**:63 (1975); D. J. Thouless, *Phys. Rep.* **13C**:94 (1974); T. Verheggen, *Commun. Math. Phys.* **68**:69 (1979); R. Cardona, *Duke Math. J.* **49**:191 (1982).
9. H. Schwerdtfeger, *Geometry of Complex Numbers* (University of Toronto Press, Toronto, 1962).